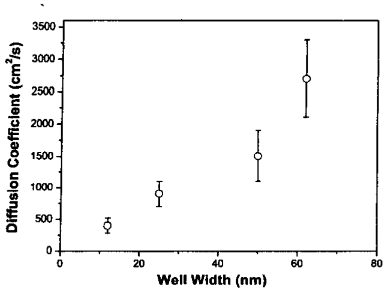

CTuW4 Fig. 3. Measured 2D diffusion coefficient vs. InGaN MQW well-width.

decrease was observed. 2D lateral diffusion coefficient D was found to increase drastically from $400 \pm 100 cm^2/s$ to $2700 \pm 500 cm^2/s$ for well width increased from 12Å up to 62Å shown in Figure 3. This interesting behavior is similar to the "giant ambipolar diffusion constant" observed in GaAs/InGaAs n-i-p-i structures.[1] In thick wells, the fast 2D lateral diffusion was due to spatial separation of the charge carriers of opposite sign which resulted from the strong piezoelectric fields. Due to decomposition of the electron-hole plasma, the attractive Coulomb interaction between electrons and holes was reduced and did no longer compensate the repulsion between carriers of the same type as it did in bulk materials.

References

1. K.H. Gulden, *et al.*, "Giant ambipolar diffusion constant of n-i-p-i doping superlattices," Phys. Rev. Lett. 66, 373–376 (1991).
2. S.F. Chichibu, *et al.*, "Optical properties of InGaN quantum wells," Mat. Sci. and Eng. B59, 298–306 (1999).

CTuW5 5:45 pm

InGaAsN quantum well structures for long-wavelength lasers

Henning Riechert, *Infineon Technology, Corporate Research Photonics, D-81730 Muenchen, Germany; Email: henning.riechert@infineon.com*

We report on the growth of this material by solid source molecular beam epitaxy (MBE) using an RF-coupled plasma source to generate reactive nitrogen from N_2. Based on optical and structural characterisation we will discuss carrier localisation, nonuniformity in composition, local bonding arrangement as well as the influence of the post-growth annealing treatment commonly used for this material.

Material-related performance data of edge-emitting lasers will be given, along with a comparison of lasers based on InGaAsP and on InGaAsN. For optimised InGaAsN structures, a decrease of single QW transparency current density down to 100 A/cm^2 has been achieved and SQW lasers with threshold current densities as low as 400 A/cm^2 for 1000 µm long, as-cleaved resonators have been made. This represents clearly the lowest laser thresholds reported so far for emission around 1.3 µm from the InGaAsN material system. Based on our results, further potential for material optimisation will be discussed.

Finally, we will present results for InGaAsN-based VCSELs on GaAs, emitting more than 0.5 mW near 1.3 µm in cw operation at 25°C.

CTuW6 6:15 pm

The effect of Mg diffusion on the contact resistance of low doped p-GaN

C.C. Chen, J.L. Yen, and Y.J. Yang, *Department of Electrical Engineering, National Taiwan University, Taipei, Taiwan; Email: yjyang@cc.ee.ntu.edu.tw*

In recent years III-nitride semiconductors have been studied intensively due to its important applications of the short-wavelength optoelectronics and electronics. Although the rapid progress on this material system already makes the commercial laser diodes (LDs) available,[1] still, the critical issue for the device is the lifetime. One of the factors affecting the lifetime is the high p-type contact resistance of the devices, which generates ohmic heating preventing the devices from cw or long-life operation. The obstacles of making a low resistance p-type contact to GaN are mainly in the difficulty to obtain a high in-situ doping level in p-GaN, and the lack of a metal with a large work function to eliminate or reduce the band offset. For the latter issue, various metals and annealing conditions were attempted to reduce the p-type contact and some good results have been achieved.[2] However, for the former issue, the doping levels in p-GaN are mostly limited to the growth systems and techniques used. Besides few reports, the maximum hole concentration in p-GaN is typically $\sim 5 \times 10^{17} cm^{-3}$, which is about two orders of magnitude lower than that of the conventional III-V semiconductors such as GaAs for making a good p-type contact. The post-growth diffusion, which is a conventional way to increase the doping level of as-grown materials, has been unavailable for GaN until recently.[3] In this letter we report for the first time that Mg diffusion was applied to low doped GaN ($\sim 3 \times 10^{16} cm^{-3}$) using Mg_3N_2 as Mg source to reduce the resistance of contact to p-GaN. The results have consistently showed a reduction of contact resistance by ~1.5 orders of magnitude.

A MOCVD grown p-GaN wafer with a hole concentration of $3 \times 10^{16} cm^{-3}$ and a thickness of ~2 µm was used for this study. To conduct the Mg diffusion into p-GaN, the sample was sealed with Ma_3N_2 powder in a vacuumed quartz ampoule and put into a 950°C for 5 min for annealing. Secondary ion mass spectroscopy (SIMS) was used to determine the Mg diffusion profile. Hall measurement was used to characterize the hole concentrations of the sample before and after diffusion. To understand the effect of surface treatment on the contact to p-GaN, the samples were also processed with and without 20 min Aqua regia etching for comparison. A Ni/Au film was deposited on the sample and annealed at 600°C for 1 min to form an ohmic contact. The contact resistance was measured by a transmission line model (TLM) using a linear configuration of 200 × 80 μm^2 metal pads with spacing varied from 4 to 40 µm linearly in 10 steps.

The measured hole concentration of the p-GaN sample increased from $3 \times 10^{16} cm^{-3}$ to $3 \times 10^{17} cm^{-3}$ after Mg diffusion. Since the diffusion region with the Mg concentration $>5 \times 10^{19} cm^{-3}$ observed from SIMS was only ~0.2 µm thick, based on a ~2 µm thick p-GaN layer, the actual hole concentration near the surface of GaN can be estimated to be $>3 \times 10^{18} cm^{-3}$, which was one order higher than the typical maximum hole concentration obtained from the in-situ doping in crystal growth. Fig. 1 shows the current-voltage (I–V) curves of the Ni/Au contacts to p-GaN wafers under four different process conditions: the as-grown as well as the diffused samples each with and without surface treatment (Aqua regia etching). It clearly indicates that the resistance of the diffused samples was much lower than that of the as-grown samples. There is a turn-on of ~1 V on the I–V curve of the diffused samples without surface etching, indicating the existence of oxide on the GaN surface.[4] With the Aqua regia etching to remove the oxide a linear I-V curve showing an ohmic contact was obtained.

Fig. 2 shows the results of the TLM measurement on the four different wafers same as those used in Fig. 1. The contact resistance was determined to be 2.73 Ω-cm^2 for the as-grown wafer, 6.86×10^{-2} Ω-cm^2 for the as-grown wafer with surface treatment, and 1.93×10^{-3} Ω-cm^2 for the diffused wafer with surface treatment respectively. These results indicate that the contact resistance was reduced by ~1.5 orders of magnitude by the surface etching only,[4] and improved by another ~1.5 orders of magnitude by the Mg diffusion. The improvement from the Mg diffusion can be explained as the following model: Since the transport property of the metal-semiconductor contact is dominated by the tunneling mech-

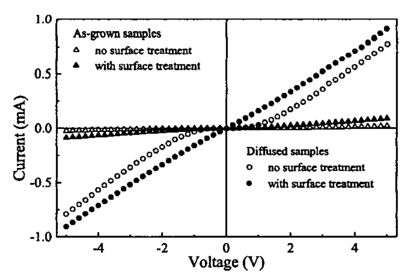

CTuW6 Fig. 1. Current-voltage curves of the samples processed under four different conditions.

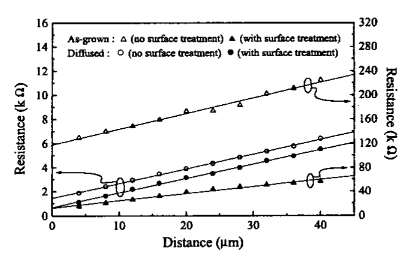

CTuW6 Fig. 2. Contact resistance measured by the transmission line model on the four different samples as same as those used in Fig. 1.

anism, the contact resistance R_c can be determined from the equation[5]

$$R_c \sim \exp\left(\frac{2\phi_B}{\hbar}\sqrt{\frac{\varepsilon_s \cdot m^*}{N_A}}\right)$$

Thus the high acceptor doping level (N_A of $>3 \times 10^{18}$ cm^{-3} resulted from the Mg diffusion into p-GaN will significantly reduce the contact resistance.

In conclusion, the Mg diffusion into low doped GaN indeed improved the Ni/Au contact to the p-GaN with a resistance reduction of ~1.5 orders of magnitude by increasing the doping level near the surface to $>3 \times 10^{18}$ cm^{-3}. This new process in conjunction with an optimized metalization will provide a reliable way to make a low resistance contact to p-GaN, which plays an important role of fabrication of high quality and long life GaN based devices.

References

1. S. Nakamura, M. Senih, S. Nagaham, N. Iwasa, T. Yamada, T. Matsushita, Y. Sugimoto, and H. Kiyoku, "Room-temperature continuous-wave operation of InGaN multi-quantum-well-structure laser diodes with a long lifetime," Appl. Phys. Lett. **70**, 868–870 (1997).
2. J.-S. Jang, S.-J. Park, and T.-Y. Seong, "Metalization scheme for highly low-resistance, transparent, and thermally stable ohmic contacts to p-GaN," Appl. Phys. Lett. **76**, 2898–2900 (2000).
3. J.L. Yen, K.W. Wen, Y.J. Yang, and C.Y. Lin, "p-type GaN formed by Mg diffusion using Mg_3N_2 as the Mg source", 25th International Conference on the Physics of Semiconductors, (Osaka, Japan, September 2000), p.934.
4. J.K. Kim, J.-L. Lee, J.W. Lee, H.E. Shin, Y.J. Park, and T. Kim, "Low resistance Pd/Au ohmic contacts to p-type GaN using surface treatment", Appl. Phys. Lett. 73, 2953–2955 (1998).
5. S.M. Sze, *Physics of Semiconductor Devices*, *2nd* ed., (Wiley, New York, 1981), p. 304.

CTuX — 4:45 pm–6:15 pm
Room 324/326

Pulsed Fiber Sources

Stojan Radic, *Bell Labs., Lucent Tech., USA, Presider*

CTuX1 — **4:45 pm**

The quantum limit of timing jitter in actively mode-locked soliton fiber lasers

M.E. Grein, H.A. Haus, E.P. Ippen, Y. Chen,* *Department of Electrical Engineering and Computer Science, and Research Laboratory of Electronics, Massachusetts Institute of Technology, 77 Massachusetts. Ave, Rm. 36-325, Cambridge, Massachusetts 02139, USA; Email: megrein@mit.edu; *Sycamore Networks, Optics Department, 4 Omni Way, Chelmsford, MA 01824-4111, USA, Tel (978) 367-7054, Fax (978) 250-3350*

The demand for stable, actively mode-locked fiber laser (AMLFL) sources with extremely small timing jitter has been driven by the development of high-speed optical communications systems and high-resolution optical sampling. Timing jitter degrades bit-error rates in the former and leads to sampling errors in the latter. AMLFL's have been shown to exhibit very low timing jitter whose performance is limited by the phase noise of the external oscillator.[1–2] In this paper, we determine the quantum-limited timing jitter of the AMLFL operating at GHz repetition rates and how it can be reduced.

At present, there are two basic types of modulation employed in the active mode-locking of fiber lasers: amplitude (AM) and phase modulation (PM). A schematic of an 80 m polarization-maintaining fiber ring laser cavity that can be configured for either AM or PM at 10 GHz is given in Fig. 1. The laser produces a train of picosecond soliton pulses whose characteristics using either modulation are similar.[3–5] However, it has been shown that the physics of pulse retiming are qualitatively different for AM and PM.[3] For AM, timing fluctuations are damped out by the amplitude modulator. For PM, mistimed pulses are first frequency shifted by the phase modulator. The frequency shifts are then converted to retiming shifts via group-velocity dispersion (GVD), and the timing restoration will depend on the product of the frequency shift exerted by the modulator and GVD. We should expect, then, that the resulting timing jitter for AM and PM are quite different, and we show in this paper that they are.

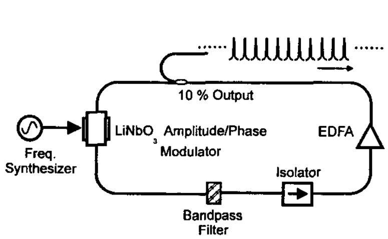

CTuX1 Fig. 1. Fiber laser configuration with filtering, isolator, erbium-doped fiber amplifier, output coupler, and a $LiNbO_3$ modulator for amplitude or phase modulation driven synchronously by a frequency synthesizer. Laser parameters are GVD D = 0.32 ps^2; modulation depth $M_{AM} = 1.0$, $M_{PM} = \pi$; filter $\Omega_f = 5.5$ nm, round-trip time $T_R = 400$ ns, pulsewidth $\tau = 1.0$ ps, unsaturated gain $g_s = 0.8$, pulse energy $w_0 = 1.0$ pJ.

The analysis is carried out using the linearized soliton perturbation theory[6] to derive analytical equations of motion for the pulse timing driven by the amplified spontaneous emission (ASE). A more general technique that can handle pulse trains of various shapes (i.e, non-solitonic) has been presented elsewhere.[7] The resulting spectrum of the timing jitter for AM is given in Fig. 2a. The spectrum has two components: the first results from a direct displacement of the pulse via ASE and is reduced by using large modulation depth. The second is due to carrier frequency displacement via ASE that couples to the timing jitter through GVD (the Gordon-Haus effect) and is reduced by filtering and small GVD. The jitter (found by integrating the jitter spectrum) is shown in Fig. 3 and is proportional to $D^2\Omega_f^4$ (where the gain of the EDFA is adjusted to keep the pulse energy constant at 1 pJ).

For the case of PM, we find that the spectrum of the jitter is more complicated and resembles that of a damped harmonic oscillator with a characteristic frequency that is proportional to $\sqrt{(M_{PM}\omega_m{}^2 D)}$ and a damping rate proportional to $(\Omega_f^2\tau^2)^{-1}$. The jitter spectrum also has two components. The first component due to direct displacements of the pulse via ASE can be reduced by increasing GVD while also increasing the filtering (overdamped), as shown in Fig. 2b. Fig. 2c shows the enhancement of the jitter spectrum if the filtering is weak (underdamped). The second component of the spectrum (Gordon-

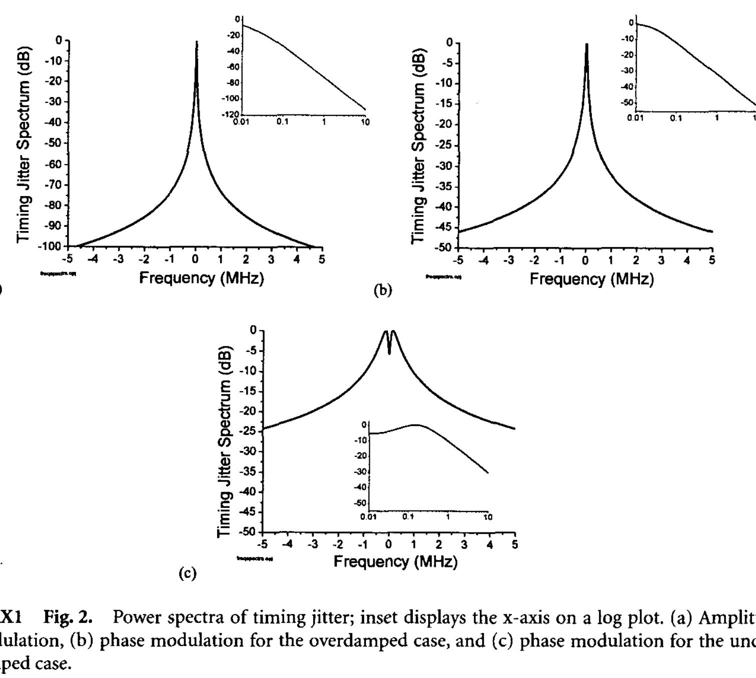

CTuX1 Fig. 2. Power spectra of timing jitter; inset displays the x-axis on a log plot. (a) Amplitude modulation, (b) phase modulation for the overdamped case, and (c) phase modulation for the underdamped case.